Ingenieur-Archiv 59 (1989) 197–208

Ingenieur-Archiv

Gradient dependent dilatancy and its implications in shear banding and liquefaction*

I. Vardoulakis, Minneapolis and **E. C. Aifantis,** Houghton

Summary: A gradient dependent dilatancy condition is assumed in order to capture the heterogeneous character of deformation in granular soils. This assumption is incorporated into the structure of classical deformation and flow theories of plasticity and its implications in two interesting examples of patterning instability, that is shear banding and liquefaction, are examined. Shear banding is considered within a modified gradient dependent deformation theory, while liquefaction is studied within a modified gradient dependent flow theory of plasticity. In both cases a deformation induced length scale is obtained near the instability, and this is identified with the thickness of the shear band or the spacing of the liquefying strips.

Gradientenabhängige Dilatanzbeziehung und ihre Implikationen auf Scherfugenbildung und Verfestigung in Böden

Übersicht: Lokale Inhomogenitäten bei der Verformung granularer Materialien sind hier mit Hilfe einer gradientenabhängigen Dilatanzbeziehung beschrieben. Diese Annahme ist in die Struktur einer klassischen Deformations- und Fließtheorie der Plastizität eingebaut, und die hiermit einhergehenden Konsequenzen werden anhand zweier interessanten Fälle der Musterbildung in Böden, nämlich Scherfugenbildung und Verflüssigung, studiert. Scherfugenbildung ist innerhalb einer modifizierten gradientenabhängigen Deformationstheorie untersucht, wogegen Bodenverflüssigung innerhalb einer modifizierten Fließtheorie analysiert wird. In beiden Fällen bekommt man in der Umgebung des Instabilitätszustandes einen deformationsinduzierten Längenmaßstab, der sich als Scherfugendicke oder als Abstand der verflüssigten Bodenstreifen manifestiert.

1 Introduction

While current work in soil mechanics emphasizes the role of finer constitutive features in predicting the critical conditions for the onset of bifurcation and localization of deformation, it does not pay much attention to the problem of capturing the evolving deformation patterns in the postlocalization regime where nonlinearities and nonconvexities (softening) may lead to serious mathematical difficulties including ill-posedness of the governing equations. This is not too surprising since the majority of the existing constitutive theories for soils are designed for describing nearly homogeneous deformations occurring in the hardening regime, rather than heterogeneous ones most pronounced in the softening regime. Naturally, soil plasticity theories have not been equipped with an internal length and, as a result, they cannot capture the heterogeneity of plastic flow in earth materials; for example, the width of the localized deformation zone in shear banding (e.g. Rudnicki and Rice [1], Vardoulakis [2], Vermeer [3], Molenkamp [4]), or the spacing of the periodic deformation patterns in stability of dilatant hardening and liquefaction problems (e.g. Rice [5], Vardoulakis [6]).

Motivated by the work of higher order diffusion theories (Aifantis [7]) and the concept of coexisting normal and excited material states (Aifantis [8]), higher order strain gradients were

* Presented at the workshop on Limit Analysis and Bifurcation Theory, held and the University of Karlsruhe (FRG), Febr. 22–25, 1988

properly introduced into a few classes of standard constitutive behavior, illustrating the ability of the gradient approach to provide characteristic lengths of deformation patterns for both metal (Aifantis [8—10]) and soil (Aifantis [11], Zbib and Aifantis [12]) mechanics problems. Emphasis, however, was placed in metals (Triantafyllidis and Aifantis [13], Zbib and Aifantis [14]) due to the existence of sufficient experimental data or clearly reproducible observations in the microscope, and only suggestive arguments were provided for corresponding soil and rock mechanics problems (Aifantis [11]).

The purpose of this paper is to further examine the role of higher order gradients in soil plasticity. Instead of introducing the gradient effect into the yield condition (Aifantis [10], Zbib and Aifantis [12]), we incorporate it into the dilatancy constraint. We then consider the resultant modifications into the deformation theory of plasticity and use such a modified theory in predicting the thickness of the shear band in a soil specimen under biaxial compression. The implications of the gradient dependent dilatancy condition into the flow theory of plasticity are also considered for both upper- and lower-bound comparison solids and their consequences to a proper wavelength selection analysis in liquefaction are discussed.

Even though our results are not complete, in the sense that only linear stability arguments are utilized and the nonlinear regime is not investigated, it is felt to present them in order to bring the problem into the attention of active workers in the field. In this connection, a more elaborate paper is being currently prepared by the authors describing the general structure of a soil plasticity theory with a gradient dependent dilatancy condition, providing a micromechanical justification of the origin of the higher order gradients for granular soils, and considering a number of applications ranging from shear band thickness and spacing of liquefying strips to wave number selection of surface instability and bore hole stability problems. In the same paper, a rather detailed comparison of the gradient approach to the Cosserat theory discussed by Mühlhaus [15] and Mühlhaus and Vardoulakis [16], which also provides an internal length scale, will be given. (More details on the Cosserat continuum approach can be found in the papers of Mühlhaus [22] and Vardoulakis [23].)

2 Motivation for higher order gradients

Even though bifurcation and spatially periodic phenomena are commonly observed at various scales in earth materials and have puzzled applied scientists and engineers for many years, there is no satisfactory theory available for their prediction and interpretation. Among these phenomena we single out faulting and surface instabilities, shear banding and progressive failure, splitting failure, and liquefaction. Careful laboratory experiments and field observations suggest that spatial periodicity with a characteristic wavelength leading to a consistently reproducible pattern formation is indeed the underlying common feature in all these phenomena. Nevertheless, this central aspect is largely ignored due to lack of proper theoretical tools and related experimental work.

The main difficulty is due to the fact that classical theories of soil plasticity do not possess an internal length scale and they break down in the post-bifurcation regime leading to mathematical problems which are either ill posed or of changing type (from elliptic to hyperbolic). The loss of ellipticity in the equilibrium equations approach, although adequate for predicting the direction of shear bands or liquefying strips and the corresponding critical stress levels, leaves the size and spacing of the localized zones unspecified. This has manifested itself quite dramatically in the numerical analysis of large scale problems where one often encounters a critical dependence of the solutions on mesh size, accompanied by stability and convergence problems. This state of affairs resulting from the absence of a characteristic length and the loss of ellipticity in the equilibrium equations renders, for example, questionable existing finite element codes for earthquake induced liquefaction and shear band induced progressive failure. In addition, physically observed features such as shear band thickness, periodicity of shear bands, and preferred wavelengths in surface instability and liquefaction phenomena cannot be modelled. The missing link in the traditional treatment of all these phenomena is the absence of an internal length scale which must be taken into account in any physical (centrifuge) or numerical (finite element) modelling. Instead, the

main effort in theoretical soil mechanics has been directed towards the mathematical description of a plethora of second order constitutive effects such as non-coaxiality, anisotropic hardening, and cyclic hardening through phenomenological generalizations of constitutive equations appropriate to locally homogeneous deformations only.

As opposed to this trend we now propose to maintain the classical structure of soil plasticity for locally homogeneous deformations (e.g. Mohr-Coulomb, non-associate, elasto-plastic model), but introduce higher order gradients approximating the heterogeneous character of the evolving microstructure in the post-bifurcation regime. Thus, the point of view is advanced here that an important class of soil behavior such as shear banding and liquefaction can only be modelled by capturing the heterogeneity of deformation and related internal flow rather than further refining constitutive equations for homogeneous deformations. In fact, the increasing complexity of homogeneous constitutive models has made it impossible to assess with reasonable accuracy their shortcomings. In this connection, we point out that the experimental data used for the calibration and validation of these models are assumed to correspond to locally or globally homogeneous deformations whereas, in fact, bifurcation and pattern formation may have already occurred, thus rendering the corresponding analyses questionable.

The need for introducing higher order gradients can also be concluded from the fact that localization of deformation in granular soils results to extreme rarefaction (dilatancy) which, in turn, is manifesting itself to material softening. Material softening (non-convexity) aggravates ill-posedness as demonstrated, for example, by Sandler and Wright [17] and Wu and Freund [18] who critically discussed the stabilizing effect of viscosity. Rate dependence should be viewed, however, as a second order effect in granular materials which are not in the rapid flow regime. This brings us naturally to the nonlinear gradient approach utilized by Aifantis and Serrin [19] in discussing non-convex equations of state and the existence of corresponding phase transition solutions. The stabilizing role of higher order gradients resulted to the obtaining of structured or bell-like solutions even for material states in the softening regime. This led Aifantis [8, 9] and subsequently Triantafyllidis and Aifantis [13] as well as Zbib and Aifantis [14] to introduce second order strain gradients in the flow stress, the strain energy function is hyperelastic materials, and the yield condition of rigid plastic materials, respectively. This, among other things, allowed for solutions to localization problems with finite shear band thickness inside the softening regime without a change of the type of the governing equations (no loss of ellipticity). A recent review of the gradient approach and its implications to obtaining the structure, width, and spacing of shear bands in metals was given by Aifantis [10].

To apply the gradient approach into the localization and deformation patterning phenomena for granular soils, one can motivate himself from metal plasticity and introduce higher order strain gradients into the Coulomb yield surface $F = \tau/p - \mu$ whose gradient dependent version gives

$$\tau/p = \mu - c\,\nabla^2\gamma^p, \tag{1}$$

where p and τ are the mean pressure and shearing stress intensity, resp., μ is the mobilized friction coefficient, γ^p is the plastic shear strain intensity and c a strain-dependent phenomenological coefficient measuring the gradient effect. It turns out, however, that a more direct and convenient way to incorporate the gradient effect in soil plasticity is to include it in the dilatancy condition $\varepsilon^p = D(\gamma^p)$ which is now being modified to read

$$\varepsilon^p = D(\gamma^p) - d\,\nabla^2\gamma^p, \tag{2}$$

where ε^p is the volumetric plastic strain and the strain-dependent phenomenological coefficient d measures the influence of the gradient effect on the dilatancy condition.

A partial motivation for (2) can be found in a microscopic calculation of a higher order gradient dependent measure for the volumetric strain. Thus if u_i^* and u_i denote the displacement vectors of two adjacent granules in a two-dimensional soil space, a Taylor's expansion yields

$$\Delta u_i = u_i^* - u_i = 2Ru_{i,j}n_j + \frac{1}{2}(2R)^2 u_{i,jk}n_jn_k + \frac{1}{6}(2R)^3 u_{i,jkl}n_jn_kn_l, \tag{3}$$

where R denotes the average radius of the grains and n_i the unit vector normal to the surface of contact. If $f(\theta)$ is an angular distribution function for the number of contacts, then the average

plastic volumetric strain is given by the expression

$$\varepsilon^p = \left(\frac{2}{\pi}\right)^2 \frac{1}{2\pi R} \int_0^{2\pi} \Delta u_i n_i f(\theta)\, \mathrm{d}\theta. \tag{4}$$

Combination of (3) and (4) and use of the identities $\overline{n_i n_j} = \delta_{ij}\pi^2/2$, $\overline{n_i n_j n_k} = 0$, $\overline{n_i n_j n_k n_l} = (\delta_{ij}\delta_{kl} + \delta_{ik}\theta_{jl} + \delta_{il}\delta_{jk})\,\pi^2/8$ with the bars denoting statistical averages, yields the expression

$$\varepsilon^p = u_{k,k} + \frac{1}{2} R^2 u_{k,kll}. \tag{5}$$

But $u_{k,k}$ denotes the usual measure of the volumetric strain and if, in seeking a generalization of (5), the factor 1/2 is replaced by an unspecified dimensionless coefficient to be determined by experiment, then an approximate Fourier transform type argument can be utilized to render the postulated gradient dependent dilatancy condition (2).

In what follows we retain (2) and assume, in addition, that the coefficient d is given by $d = L^2 D''$ where L is an internal characteristic length scale (e.g. grain size) and the prime denotes derivative of a function with respect to its argument. Then, the incremental form of (2) reads

$$\dot{\varepsilon}^p = \overline{\beta}(\gamma^p)\,\dot{\gamma}^p, \qquad \overline{\beta} = \beta(\gamma^p) - L^2\beta'\,\nabla^2\dot{\gamma}^p/\dot{\gamma}^p \tag{6}$$

where $\beta \equiv D'$ is the usual dilatancy function and the assumption of nearly homogeneous ground states ($\nabla\gamma^p \simeq 0$) was used. Equation (6) is the new ingredient that we will utilize in our analysis, the remaining of the structure being as in classical soil plasticity developments. For the deformation theory of plasticity, the resultant modifications can be clearly seen in the next section where shear band bifurcation and thickness can be analyzed. For the flow theory of plasticity, the resultant modifications will be seen in the last section where a wavelength analysis for pattern selection in liquefaction will be provided. As the concepts of upper- and lower-bound linear comparison solids are important in this analysis, we summarize here the appropriate constitutive equations (see also Vardoulakis [20]).

The upper-bound linear comparison solid is defined by the following expressions between the stress- and the strain-rate tensors (we adopt the usual additivity assumption $\dot{\varepsilon}_{ij} = \dot{\varepsilon}^e_{ij} + \dot{\varepsilon}^p_{ij}$ $(i, j = 1, 2)$ and the standard notation for the elastic constants G, K and ν)

$$\dot{\sigma}_{ij} = G L_{ijkl}\dot{\varepsilon}_{kl} = G(L^e_{ijkl} - L^p_{ijkl})\,\dot{\varepsilon}_{kl}, \tag{7}$$

where

$$\begin{aligned} &L^e_{ijkl} = (\alpha - 1)\,\delta_{ij}\delta_{kl} + 2\delta_{ik}\delta_{jl}, \qquad \alpha = K/G = 1/(1 - 2\nu), \\ &L^p_{ijkl} = A^Q_{ij}A^F_{kl}/H, \qquad A^Q_{ij} = s_{ij}/\tau + \alpha\beta\delta_{ij}, \qquad A^F_{ij} = s_{ij}/\tau + \alpha\mu\delta_{ij}, \\ &H = 1 + h - h_T > 0, \qquad h = h_t p/G, \qquad h_T = -\alpha\mu\beta, \qquad h_t = \mathrm{d}\mu/\mathrm{d}\gamma^p, \end{aligned} \tag{8}$$

with

$$\begin{aligned} &p = -\sigma_{kk}/2, \qquad \tau = (s_{ij}s_{ij}/2)^{1/2}, \qquad s_{ij} = \sigma_{ij} + p\delta_{ij}, \\ &\dot{\varepsilon}^p = \dot{\varepsilon}^p_{kk}, \qquad \dot{\gamma}^p = (2\dot{e}^p_{ij}\dot{e}^p_{ij})^{1/2}, \qquad \dot{e}^p_{ij} = \dot{e}^p_{ij} + \dot{\varepsilon}^p\delta_{ij}/2, \end{aligned} \tag{9}$$

and the mobilized coefficient μ and the dilatancy function β defined as usual by the Coulomb yield surface F and the potential surface Q as

$$F = \tau/p - \mu = 0, \qquad Q = \tau/p - \beta = 0. \tag{10}$$

In general, the functions μ and β depend on both the porosity n and the plastic strain γ^p but they will be viewed here as functions of γ^p only. They both exhibit a softening regime for advanced deformations as suggested by experiment. As already mentioned, the only modification that we introduce into the classical plasticity structure is to replace β in $(10)_2$ by $\overline{\beta}$ defined in (6). In passing, we point out that the above relations also hold for a flow theory of plasticity where

loading and unloading is allowed (the linear comparison solid does not unload) by introducing the switch function $\langle 1\rangle$ in the definition of the plastic modulus so that

$$L^p_{ijkl} = \langle 1\rangle A^Q_{ij} A^F_{kl}/H,$$
$$\langle 1\rangle = \begin{cases} 1 & \text{for} \quad F = 0 \quad \text{and} \quad L^e_{ijkl}\dot{\varepsilon}_{kl}\, \partial F/\partial\sigma_{ij} > 0, \\ 0 & \text{for} \quad F < 0, \quad \text{or} \quad F = 0 \quad \text{and} \quad L^e_{ijkl}\dot{\varepsilon}_{kl}\, \partial F/\partial\sigma_{ij} \leqq 0, \end{cases} \tag{11}$$

i.e. $\langle 1\rangle = 1$ if loading of the yield surface is taking place and $\langle 1\rangle = 0$ if either the stress state is in the elastic domain or if it is on the yield surface and unloading or neutral loading is taking place. Due to the switch function $\langle 1\rangle$, the stiffness tensor L_{ijkl} is a non-linear operator. In the case of non-associate flow-rule, L_{ijkl} is non-symmetric ($L_{ijkl} \neq L_{klij}$).

The lower bound linear comparison solid is also defined by (8) with the exception that it contains an additional parameter r ($0 \leqq r \leqq 1$) which can be varied so as to maximize the lower bound estimate of the bifurcation load (Raniecki and Bruhns [21]). It turns out that the appropriate modulus is given by the relation

$$L_{ijkl} = L^e_{ijkl} - \frac{1}{4rH}\,(A^Q_{ij} + rA^F_{ij})\,(A^Q_{kl} + rA^F_{kl}), \quad r^2 = \frac{1 + \alpha\beta^2}{1 + \alpha\mu^2}, \tag{12}$$

and it should be noticed that the stiffness matrix for this linear comparison solid is symmetric. If an associate flow-rule is assumed ($F \equiv Q, \mu = \beta$), then the two linear comparison solids coincide for $r = 1$, and the bifurcation load obtained from a linear bifurcation analysis coincides with the true bifurcation load.

In the coordinate system of principal directions of the initial stress, the rate constitutive equations for the two comparison solids can easily be derived from the above general expressions (7) and (8) or (12) resulting to the equations

$$\dot{\sigma}_{11} = G(L_{1111}\dot{\varepsilon}_{11} + L_{1122}\dot{\varepsilon}_{22}), \quad \dot{\sigma}_{22} = G(L_{2211}\dot{\varepsilon}_{11} + L_{2222}\dot{\varepsilon}_{22}), \quad \dot{\sigma}_{12} = 2G\dot{\varepsilon}_{12}, \tag{13}$$

where for the upper-bound linear comparison solid

$$\begin{aligned} L_{1111} &= [\alpha(1-\beta)\,(1-\mu) + (1+\alpha)\,h]/H, \\ L_{1122} &= [\alpha(1+\beta)\,(1-\mu) - (1-\alpha)\,h]/H, \\ L_{2211} &= [\alpha(1-\beta)\,(1+\mu) - (1-\alpha)\,h]/H, \\ L_{2222} &= [\alpha(1+\beta)\,(1+\mu) + (1+\alpha)\,h]/H, \end{aligned} \tag{14}$$

and for the lower-bound linear comparison solid

$$\begin{aligned} L_{1111} &= \alpha + 1 - \frac{1}{4rH}\,[(1+\alpha\beta) + r(1+\alpha\mu)]^2, \\ L_{1122} &= L_{2211} \\ &= \alpha - 1 + \frac{1}{4rH}\,[(1+\alpha\beta) + r(1+\alpha\mu)]\,[(1-\alpha\beta) + r(1-\alpha\mu)], \\ L_{2222} &= \alpha + 1 - \frac{1}{4rH}\,[(1+\alpha\beta) + r(1-\alpha\mu)]^2. \end{aligned} \tag{15}$$

3 Modified deformation theory — Shear banding

Let us consider a plane strain soil specimen subjected to biaxial compressive loading $\sigma_2 < \sigma_1 < 0$ ($\dot{\varepsilon}_{22} < \dot{\varepsilon}_{11}$) as shown in Fig. 1. For rigid plastic behavior ($\dot{\gamma} = \dot{\gamma}^p$), the appropriate standard stress-strain relations are (Vardoulakis [2])

$$\dot{\sigma}_{11} = (1-\mu)\,\dot{p} + G_t\dot{\gamma}, \quad \dot{\sigma}_{22} = (1+\mu)\,\dot{p} - G_t\dot{\gamma}, \quad \dot{\sigma}_{12} = 2G_s\dot{\varepsilon}_{12}, \tag{16}$$

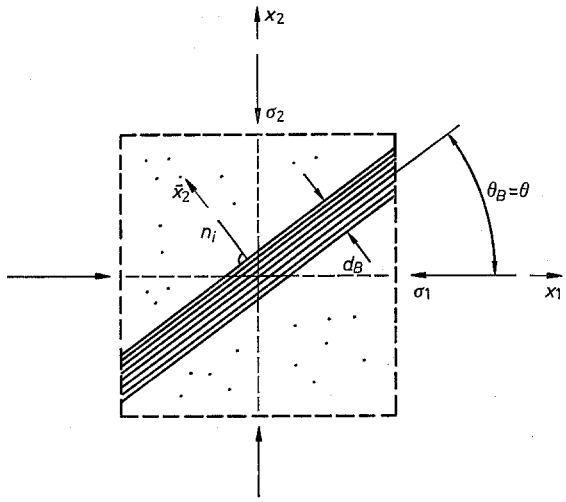

Fig. 1. Element with shear band

while the presently adopted modified (i.e. gradient dependent) dilatancy condition reads

$$\dot{\varepsilon} = \bar{\beta}(\gamma)\,\dot{\gamma}, \qquad \bar{\beta}(\gamma) = \beta(\gamma) - L^2\beta'(\gamma)\,\nabla^2\dot{\gamma}/\dot{\gamma}, \tag{17}$$

with $\tau = \mu\,|p|$ and

$$\dot{\gamma} = \dot{\varepsilon}_{11} - \dot{\varepsilon}_{22}, \quad \dot{\varepsilon} = \dot{\varepsilon}_{11} + \dot{\varepsilon}_{22}, \quad \tau = (\sigma_1 - \sigma_2)/2, \quad p = (\sigma_1 + \sigma_2)/2,$$
$$G_t = |p|\,h_t, \qquad G_s = |p|\,h_s, \qquad h_t = \mathrm{d}\mu/\mathrm{d}\gamma, \qquad h_s \equiv \mu/\gamma.$$

The corresponding equilibrium equations are

$$\begin{aligned} &\dot{\sigma}_{11,1} + \dot{\sigma}_{12,2} + (\sigma_1 - \sigma_2)\,\dot{\omega}_{,2} = 0, \\ &\dot{\sigma}_{21,1} + \dot{\sigma}_{22,2} + (\sigma_1 - \sigma_2)\,\dot{\omega}_{,1} = 0, \end{aligned} \tag{18}$$

where $\dot{\omega} = (v_{2,1} - v_{1,2})/2$ with v_i denoting the velocity field.

Upon combination of (16) and (18) we obtain for homogeneous ground states

$$\begin{aligned} -(1-\mu)\,\dot{p}_{,12}/p &= h_t v_{1,112} + (h_s - \mu)\,v_{1,222} + (h_s - h_t + \mu)\,v_{2,122} \equiv -\tilde{A}, \\ -(1+\mu)\,\dot{p}_{,21}/p &= (h_s - h_t - \mu)\,v_{1,121} + (h_s + \mu)\,v_{2,111} + h_t v_{2,221} \equiv -\tilde{B}, \end{aligned} \tag{19}$$

implying, with $\lambda^2 \equiv (1+\mu)/(1-\mu)$, the condition

$$\frac{\dot{p}_{,12}}{p} = \frac{\tilde{A}}{1-\mu} = \frac{\tilde{B}}{1+\mu} \to \lambda^2\tilde{A} = \tilde{B}. \tag{20}$$

This, in turn, leads to the relation

$$a_1 v_{1,112} + a_2 v_{1,222} - a_3 v_{2,122} - a_4 v_{2,111} = 0, \tag{21}$$

where

$$a_1 = (1+\lambda^2)\,h_t - (h_s - \mu), \qquad a_2 = \lambda^2(h_s - \mu),$$
$$a_3 = (1+\lambda^2)\,h_t - \lambda^2(h_s + \mu), \qquad a_4 = h_s + \mu.$$

Similarly, the gradient dependent dilatancy condition (17) yields

$$v_{1,1} + v_{2,2} = \beta(v_{1,1} - v_{2,2}) - L^2\beta'[(v_{1,1} - v_{2,2})_{,11} + (v_{1,1} - v_{2,2})_{,22}], \tag{22}$$

which, with $\delta^2 = (1+\beta)/(1-\beta)$ and $b = \beta'/(1-\beta)$ can be written in the form

$$L^2 b(v_{1,111} + v_{1,122} - v_{2,211} - v_{2,222}) + v_{1,1} + \delta^2 v_{2,2} = 0. \tag{23}$$

We now search for a shear band solution with $y = \pi\bar{x}_2/2l$, $q = \pi L/(2l)$, $[n_i] = [n_1, n_2] = [-\sin\theta_B, \cos\theta_B]$ and $\partial/\partial\bar{x}_1 = 0$, $\partial/\partial x_i = n_i\,\partial/\partial\bar{x}_2$ (see Fig. 1). Then, (21) and (23) give, resp.

$$\begin{aligned} &b_1 v_1''' - b_2 v_2''' = 0, \\ &q^2 b(n_1 v_1''' - n_2 v_2''') + n_1 v_1' + \delta^2 n_2 v_2' = 0 \end{aligned} \tag{24}$$

where the new coefficients b_1 and b_2 are defined by $b_1 \equiv (a_1 n_1^2 + a_2 n_2^2)\, n_2$ and $b_2 \equiv (a_3 n_2^2 + a_4 n_1^2)\, n_1$. On assuming periodic solutions of the form

$$v_i = c_i \sin y, \tag{25}$$

(24) yields

$$\begin{bmatrix} b_1 & -b_2 \\ n_1(1 - q^2 b) & n_2(\delta^2 + q^2 b) \end{bmatrix} \begin{bmatrix} c_1 \\ c_2 \end{bmatrix} = 0, \tag{26}$$

which for a non-trivial solution gives for the wave number q the expression

$$q^2 = \frac{b_2 n_1 + b_1 n_2 \delta^2}{(b_2 n_1 - b_1 n_2)\, b} = \frac{1}{b}\frac{A}{B} \tag{27}$$

where

$$A \equiv A(\theta) = \tan^4\theta + \alpha_1 \tan^2\theta + \alpha_2, \quad B \equiv B(\theta) = \tan^4\theta + \beta_1 \tan^2\theta + \beta_2, \tag{28}$$

with α_1, α_2 and β_1, β_2 defined by the relations

$$\alpha_1 = h_t(1 + \lambda^2)(1 + \delta^2)/(h_s + \mu) - \lambda^2 - \xi\delta^2, \qquad \alpha_2 = \xi\lambda^2\delta^2,$$
$$\beta_1 = \xi - \lambda^2, \qquad \beta_2 = -\xi\lambda^2, \qquad \xi = (1 - \gamma)/(1 + \gamma).$$

Even though the result (27) does not allow for a preferred wavelength selection analysis as is the case, for example, in the work of Aifantis [10] and Zbib and Aifantis [14], it does provide quite sufficient information for both the direction of the band, as well as a measure of its thickness at the very beginning stages of its development. To see that we note that the classical bifurcation analysis gives $A = 0$ which, in view of (27), implies $q = 0$ (infinite wavelength) at the onset of localization. (It turns out that $B < 0$ for $\theta < \theta_c = 45° + \varphi/2$, $\varphi = \sin^{-1}\mu$). This, in turn, leads to the familiar result of shear band inclination predicted within the classical deformation theory of soil plasticity (Vardoulakis [2]) without a gradient dependent dilatancy condition, namely, $\theta = \theta_B = 45° + (\varphi + \psi)/4$, $\psi = \sin^{-1}\beta$. This fixes the orientation of the band, say at $\theta = \theta_B$ and allows for the evaluation of a shear band thickness $d_B = 2l$ as predicted by (27) at a given state of deformation. Experimental graphs for the variation of q and l/L with the advancement of deformation are given in Fig. 2. Although the validity of these graphs may be questionable as they were constructed on the basis of a linearized theory, it is interesting to note that for a FS-03 test of Holland fine sand the shear band thickness was measured to be $d_B^{(1)} = 3.7$ mm and the corresponding failure strain $\gamma_B^{(1)} = 0.06$. This provides a value of $q_{cr} = 0.085$ and then the corresponding value of the internal length is $L = 0.1$ mm. Similarly, for a second test D-27 (medium grain Karlsruhe sand) we obtained $d_B^{(2)} = 4.3$ mm, $q_{cr} = 0.09$ and $L = 0.12$ mm. The corresponding grain size in each of the above cases is $R = 0.1$ mm and $R = 0.16$ mm, resp., and these values are remarkably close to the calculated values of the internal length L as listed above.

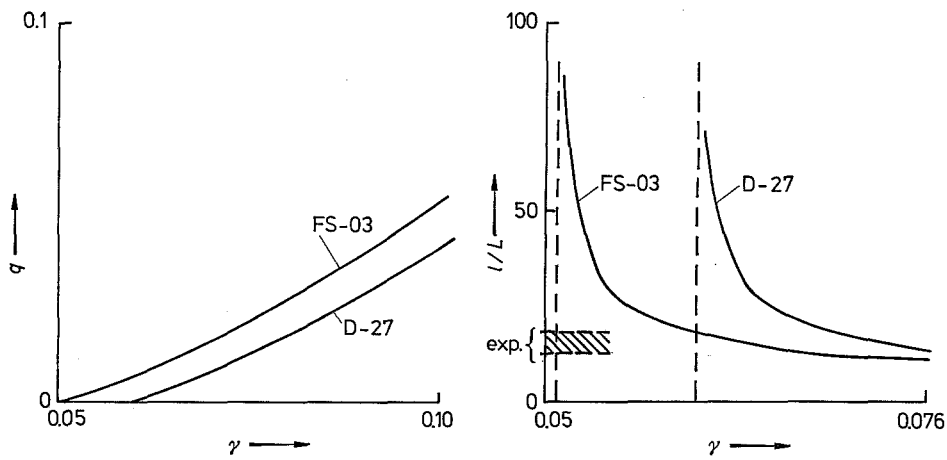

Fig. 2. Evolution of wave number and shear band thickness for two different sand specimens

4 Modified flow theory — Liquefaction

Let us consider an infinite water-saturated solid strip subjected to compressive σ_{22} (< 0) and shear σ_{12} stresses as shown in Fig. 3a. If p^w denotes the pore water pressure, then the effective stress is $\sigma'_{ij} = \sigma_{ij} - p^w \delta_{ij}$. We assume a uniform initial state of stress

$$\sigma'_{ij} = \begin{bmatrix} \sigma' & \tau \\ \tau & \sigma' \end{bmatrix},$$

and examine its stability versus small exponential fluctuations occuring during the course of rectilinear deformations of the form

$$\dot{\varepsilon}_{ij} = \begin{bmatrix} 0 & \dot{\gamma}/2 \\ \dot{\gamma}/2 & \dot{\varepsilon} \end{bmatrix},$$

where $\dot{\gamma} = v_{1,2}$ and $\dot{\varepsilon} = v_{2,2}$ with the initial value of $\dot{\varepsilon}$ vanishing (stability of undrained shear).

For dilatant rocks this problem was first studied by Rice [5] who found that the behavior of the system is governed by a diffusion equation and, thus, loss of stability occurs when the diffusivity becomes negative, a condition enforced in the softening regime. Motivated by a correction to the diffusion equation to incorporate inertia (Aifantis [7]), Vardoulakis [6] re-examined Rice's problem for contractant sands by including dynamic effects. He found that without inertia the growth coefficient has a singularity which does not appear when inertia is included. However, no wavelength selection analysis was provided in the above works mainly due to the absence of a suitable internal length in their formulation. Such an internal length was included, in the form of higher order pore pressure gradients entering Darcy's law, in the stability analysis for undrained shear given by Aifantis [11]. A similar point of view is adopted here but instead of modifying Darcy's law, we explore the possibility of a patterning instability in the undrained shear problem on the basis of the gradient dependent dilatancy condition (6).

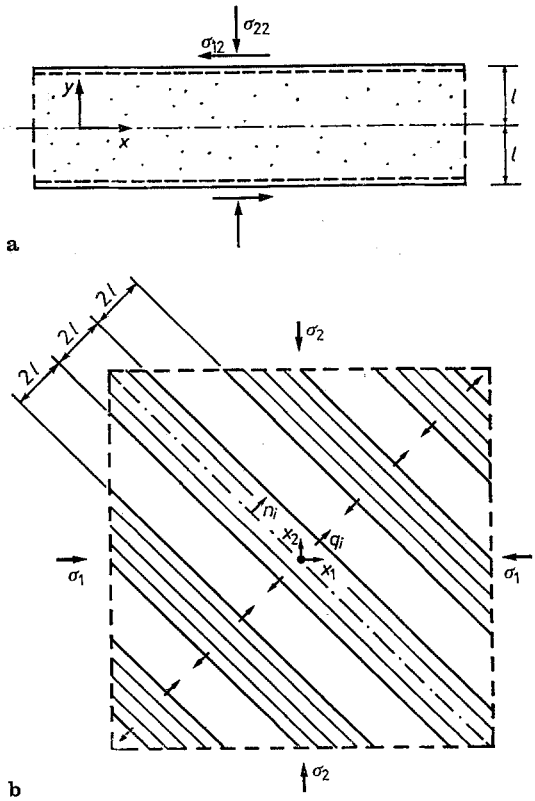

Fig. 3. a Simple shear of a saturated layer; **b** periodic configuration of contracting and dilating layers (angle $\theta_T = \pi/4$; q_i denotes the water flow)

The relevant balance equations are given by

$$\dot{\sigma}_{12,2} = 0, \quad \dot{\sigma}'_{22,2} = \dot{p}^w_{,2}, \quad \dot{\varepsilon}_{,t} = \frac{1}{b}\,\dot{p}_{,22}, \tag{29}$$

where the first two relations are the usual equilibrium equations and the third one is Darcy's law ($b = \varrho^w \mu^w / k$, with ϱ^w denoting the water density, μ^w its viscosity and k the permeability). The corresponding constitutive equations for both the upper- and lower-bound linear comparison solids can be obtained from the general constitutive equations of Sect. 2. They read

$$\begin{aligned} \dot{\sigma}_{12}/G &= \frac{1}{H}\left[(h - h_T)\,\dot{\gamma} - \alpha\mu\dot{\varepsilon}\right] - \frac{\alpha}{H}\,\mu\beta' L^2 \dot{\gamma}_{,22}, \\ \dot{\sigma}'_{22}/K &= \frac{1}{H}\left[-\beta\dot{\gamma} + \left(1 + h + \frac{1}{\alpha}\,H\right)\dot{\varepsilon}\right] + \frac{1}{H}\,\beta' L^2 \dot{\gamma}_{,22}, \end{aligned} \tag{30}$$

for the modified upper-bound solid, and

$$\begin{aligned} \dot{\sigma}_{12}/G &= \frac{1}{H}\left[(h - h_T - \varrho_3^2)\,\dot{\gamma} - \alpha\varrho_1\varrho_2\dot{\varepsilon}\right] - \frac{\alpha}{H}\,\mu\beta' L^2 \dot{\gamma}_{,22}, \\ \dot{\sigma}'_{22}/K &= \frac{1}{H}\left[-\varrho_1\varrho_2\dot{\gamma} + H\left(1 + \frac{1}{\alpha} - \frac{\alpha}{H}\,\varrho_2^2\right)\dot{\varepsilon}\right], \end{aligned} \tag{31}$$

for the modified lower-bound solid. The new coefficients ϱ_1, ϱ_2, ϱ_3 are given by the relations $\varrho_{1,3} = (1 \pm r)/(2\sqrt{r})$, $\varrho_2 = (\beta + r\mu)/(2\sqrt{r})$ and the remaining of the symbols have been defined earlier in Sect. 2. Certain approximations (e.g. $\nabla^2\dot{\gamma}^p/\dot{\gamma}^p \simeq \nabla^2\gamma/\gamma$) were adopted in obtaining (30) and (31) in their final form but they are not essential in the subsequent steps of the analysis.

By combining (29) and (30) we obtain the following higher order diffusion equation for the increment of strain $\dot{\gamma}$

$$(h - h_T)\,\dot{\gamma}_{,T} = c_1 q^2 \dot{\gamma}_{,yy} - c_2 q^4 \dot{\gamma}_{,yyyy} - c_3 q^2 \dot{\gamma}_{,yyT}, \tag{32}$$

where the dimensionless coordinates y, T and wave number q are defined by $y = \pi x_2/(2l)$, $T = Kt/bL^2$, $q = \pi L/(2l)$, while the coefficients c_1 to c_3 are given by $c_1 = [h + a(h - h_T)]/(1 + h - h_T)$, $c_2 = a\alpha\mu\beta'/(1 + h - h_T)$, $c_3 = \alpha\mu\beta'$ with $a = h + H/\alpha$. It is pointed out that (32) was first obtained by Aifantis [7] in the context of non-classical viscosity and surface tension dependent diffusion in solids and a version of it was also discussed by Aifantis [11] in the context of stability of dilatant hardening. For contractant materials, which is the subject of our discussion here, it follows that $h_T > 0$ and therefore for $h - h_T > 0$, i.e. before the Tresca point, we have stability. On the other hand, for $h \leqq h_T$ the problem becomes ill-posed as the growth coefficient ω switches from $-\infty$ to $+\infty$ at $h = h_T$. To see these results we first note that the coefficients c_1 to c_3 remain always positive and that the substitution $\dot{\gamma} = \dot{\gamma}_0\, e^{\omega t} \cos y$ leads to a dispersion equation whose graph is depicted in Fig. 4. We remark that, as noted by Zbib and Aifantis [14], the singular behavior of the graph $\omega = \omega(q)$ at $q = q_{cr}$ is physically undesirable and this seems to imply a difficulty with the structure of the model.

Such a difficulty is not present if a lower-bound linear comparison solid is assumed. For such a solid, combination of the constitutive relations (31) and the balance equations (29) yields again the higher order diffusion equation

$$\dot{\gamma}_{,T} = c_1 q^2 \dot{\gamma}_{,yy} - c_2 q^4 \dot{\gamma}_{,yyyy} - c_3 q^2 \dot{\gamma}_{,yyT}, \tag{33}$$

where the same dimensionless variables as for the derivation of (32) were used. The new coefficients c_1 to c_3 are now defined by $c_1 = (c_{11}c_{22} - c_{12}c_{21})/c_{11}$, $c_2 = c^* c_{22}/c_{11}$, $c_3 = c^*/c_{11}$ where, in turn, the coefficients c_{ij} are given by

$$\begin{aligned} c_{11} &= (h - h_T - \varrho_3^2)/H, \qquad c_{12} = \alpha\varrho_1\varrho_2/H, \qquad c_{21} = \varrho_1\varrho_2/H, \\ c_{22} &= 1 + 1/\alpha - \varrho_2^2\alpha/H, \qquad c^* = \alpha\mu\beta'/H. \end{aligned}$$

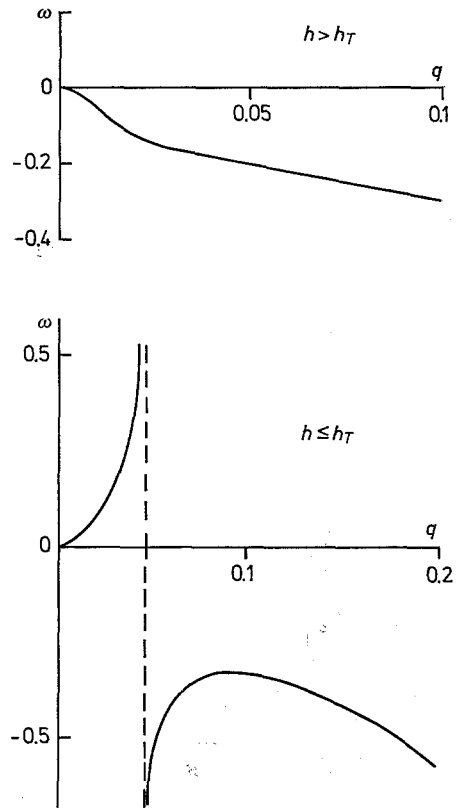

Fig. 4. Exponential growth coefficient of shear strain rate versus wave number for lower-bound comparison solid

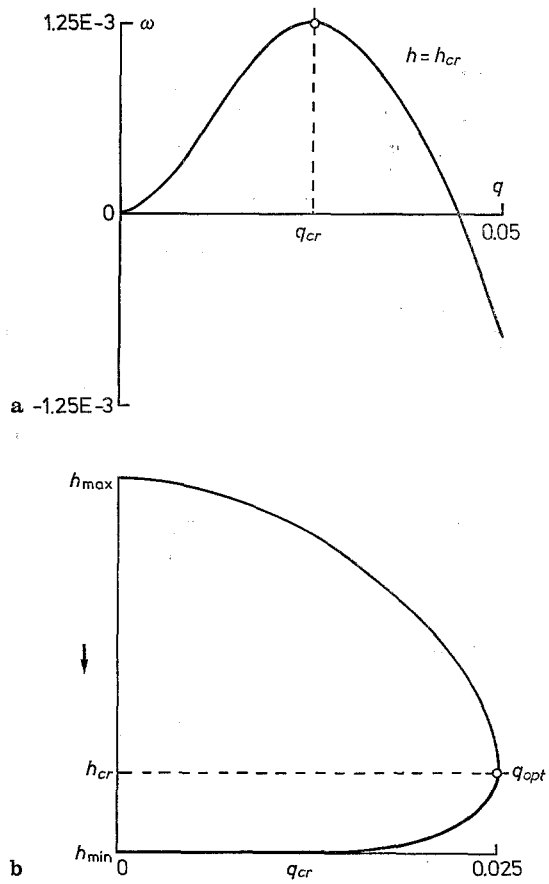

Fig. 5. Upper-bound comparison solid. **a** Exponential growth coefficient of shear strain rate versus wave number; **b** preferred wave number versus h (see (8))

On searching again for the growth or decay of exponential fluctuations of the form $\dot{\gamma} = \dot{\gamma}_0 e^{\omega t} \cos y$, we obtain the same form of the dispersion equation $\omega = \omega(q)$ as in the case of (32). It reads

$$\omega = -(c_1 + c_2 q^2)\, q^2/(1 + c_3 q^2). \tag{34}$$

The first instability occurs when $c_1 = 0$ implying $\det [c_{ij}] = 0$, while ill-posedness occurs when $c_3 = 0$ implying $c_{11} = 0$. In the first case we obtain $h = h_{\max} = h_T + \varrho_3^2 + [\alpha^2/(1 + \alpha)]\, \varrho_2^2$ and in the second $h = h_{\min} = h_T + \varrho_3^2$. The preferred wave number q_{cr} is obtained by maximizing ω in (34), that is by setting $\partial\omega/\partial q = 0$, leading to an essential quadratic equation $c_2 c_3 q_{cr}^4 + 2 c_2 q_{cr}^2 + c_1 = 0$ whose roots determine q_{cr}. These results are depicted in Fig. 5. It is noted that the drawing in Fig. 5b is somewhat exaggerated as it clearly corresponds to the nonlinear regime $h_{\min} < h < h_{\max}$. Nevertheless, it may be suggestive, perhaps, of the optimum wave number selected by the system when the assertion is being made that states in the regime $h_{\min} < h < h_{\max}$ can still be approximately described by the present equation. It is emphasized that this is the first time that a detailed and rather satisfactory wavelength analysis is presented in connection with the liquefaction instability, giving an appropriate spacing for the liquefying strips. The direction of the liquefying strips is predicted as in the classical bifurcation analysis and is not affected by the higher order terms. This gives $\theta_T = \pi/4$, a result that can be derived in a manner similar to that obtained for the direction of the shear band $\theta_B = (\pi + \psi + \varphi)/4$ discussed in the previous section (see Fig. 3b).

The derivation of the higher order diffusion equation for the plastic strain increment $\dot{\gamma}$ within the gradient approach, has motivated the attempt to search for an analogous result within the Cosserat approach. Remarkably, it turned out that the same equation (33) for the Cosserat spin w^s can formally be obtained. Even though it may be argued that within the linearized regime several generalized continuum theories may lead to similar dispersion equations, it is planned to discuss these results in a separate paper where a detailed comparison between the two approaches will be made.

5 Conclusions

We have demonstrated that the essential features of pattern formation in granular soils can be captured by a suitable modification of the dilatancy condition to include higher-order strain gradients. The discussion was based on linear stability analysis. The new feature that distinguishes the present work from previous bifurcation studies in the soil literature is the wave selection analysis and emphasis on spatial aspects. It was thus possible to obtain estimates for the width of the shear band and the spacing of liquefying strips at the initial stages of the process. In order to be able to capture, however, the evolution of the shear band thickness in the softening regime, and the subsequent configuration of the liquefaction pattern, a nonlinear analysis along the lines followed by Aifantis and co-workers [10, 13, 14] should be adopted.

Acknowledgements

Support of the National Science Foundation under grants ES-8800381(IV) and CES-8800459 (ECA) is gratefully acknowledged.

References

1. Rudnicki, J. W.; Rice, J. R.: Conditions for the localization of the deformation in pressure-sensitive dilatant materials. J. Mech. Phys. Sol. 23 (1975) 371–394
2. Vardoulakis, I.: Shear band inclination and shear modulus of sand in biaxial tests. Int. J. Num. Anal. Meth. Geomech. 4 (1980) 103–119
3. Vermeer, P. A.: A simple shear band analysis using compliances. In: Vermeer, P. A. et al. (eds.) JUTAM Conf. on deformation and failure of granular materials, pp. 493–499. Rotterdam: Balkema 1982
4. Molenkamp, F.: Comparison of frictional material models with respect to shear band initiation. Geotechnique 35 (1985) 127–143
5. Rice, J. R.: On the stability of dilatant hardening for saturated rock masses. J. Geophys. Res. 80 (1975) 1531–1536

6. Vardoulakis, I.: Dynamic stability analysis of undrained simple shear on water-saturated granular soils. Int. J. Num. Anal. Meth. Geomech. 10 (1986) 177—190
7. Aifantis, E. C.: On the problem of diffusion in solids. Acta Mech. 37 (1980) 265—296
8. Aifantis, E. C.: On the microstructural origin of certain inelastic models. Trans. ASME J. Mat. Eng. Tech. 106 (1984) 326—330
9. Aifantis, E. C.: Continuum models for dislocated states and media with microstructures. In: Aifantis, E. C.; Hirth, J. P. (eds.) The mechanics of dislocations (Proc. Int. Symp. held at Houghton, Michigan, August 28—31, 1983), pp. 127—146. Metals Park: ASM 1985
10. Aifantis, E. C.: The physics of plastic deformation. Int. J. Plasticity 3 (1987) 211—247
11. Aifantis, E. C.: Application of mixture theory to fluid saturated geologic media. In: Saxena, S. K. (ed.) Compressibility phenomena in subsidence (Proc. of the Engineering Foundation Conf. held at Henniker, New Hampshire, July 29—August 3, 1984), pp. 65—78. New York: Engng. Foundation 1986
12. Zbib, H. M.; Aifantis, E. C.: Instabilities in metals and geomaterials. A gradient approach. In: Steele, C. R.; Bevilacqua, L. (eds) I Pan American Congress of Appl. Mech. (PACAM), pp. 532—535. Rio de Janeiro: PUC-RIO 1989
13. Triantafyllidis, N.; Aifantis, E. C.: A gradient approach to localization of deformation — I. Hyperelastic materials. J. Elasticity 16 (1986) 225—238
14. Zbib, H. M.; Aifantis, E. C.: On the localization and postlocalization behavior of plastic deformation: I. On the Initiation of shear bands; II. On the evolution and thickness of shear bands; III. On the structure and velocity of the Portevin-Le Chatelier bands. Res. Mechanica 23 (1988) 261—277, 279—292, 293—305
15. Mühlhaus, H. B.: Scherfugenanalyse bei granularem Material im Rahmen der Cosserat-Theorie. Ing. Arch. 56 (1986) 389—399
16. Mühlhaus, H.-B.; Vardoulakis, I.: The thickness of shear bands in granular materials. Geotechnique 37 (1987) 271—283
17. Sandler, I. S.; Wright, J. P.: Strain softening. In: Nemat-Nasser, S. et al. (eds.) Mechanics of elastic and inelastic solids 6 (Proc. workshop on theoretical foundation for large-scale computations of non-linear material behavior), pp. 285—296. Dordrecht: Martinus-Nijhoff 1984
18. Wu, F. J.; Freund, L. B.: Deformation trapping due to thermoplastic instability in one dimensional wave propagation. J. Mech. Phys. Sol. 32 (1984) 119—132
19. Aifantis, E. C.; Serrin, J. B.: The mechanical theory of fluid interfaces and Maxwell's rule. Also: Equilibrium solutions in the mechanical theory of fluid microstructures. J. Colloid Interf. Sci. 96 (1983) 517—529, 530—547
20. Vardoulakis, I.: Theoretical and experimental bounds for shear-band bifurcation strain in biaxial tests on dry sand. Res. Mechanica 23 (1988) 239—259
21. Raniecki, B.; Bruhns, O. T.: Bounds to bifurcation stresses in solids with non-associated plastic flow law of finite strain. J. Mech. Phys. Sol. 29 (1981) 153—172
22. Mühlhaus, H.-B.: Application of Cosserat theory in numerical solutions of limit load problems. Ing. Arch. 59 (1989) 124—137
23. Vardoulakis, I.: Shear-banding and liquefaction in granular materials on the basis of a Cosserat continuum theory. Ing. Arch. 59 (1989) 106—113

Received June 27, 1988

Prof. I. Vardoulakis
Dept. of Civil and Mineral Engineering
University of Minnesota
500 Pillsbury Drive S.E.
Minneapolis, Minnesota 55455-0220, USA

Prof. E. C. Aifantis
Dept. of Mechanical Engineering and Engineering Mechanics
Michigan Technological University
Houghton, Michigan 49931
USA